Self-Condensing Atom Transfer Radical Polymerization of Inimers of Different Reactivity Ratios with Styrene and the Thermal Properties of Poly(2,6-dimethyl-1, 4-phenylene oxide)/Branched Polystyrene Blends

Guangqun Zhai, Chun Li, Yan Fang, Bibiao Jiang, Chao Jin, Hongmei Song

Division of Soft Matter and Macromolecular Science, Department of Materials Science and Engineering, Changzhou University, Changzhou 213164, China

Received 19 November 2009; accepted 28 November 2010
DOI 10.1002/app.33845
Published online 30 March 2011 in Wiley Online Library (wileyonlinelibrary.com).

ABSTRACT: Although the self-condensing atom transfer radical polymerization (SCATRP) of inimers with typical comonomers has been extensively performed, there have been few reports to correlate the reactivity ratio with the growth of the molecular weights (MWs) and the development of branched structures. Thus, the SCATRP of inimers of different reactivity ratios, namely, 4-chloromethylstyrene (CMS) and maleimide (MI) inimers, with a large excess of styrene (St) were carried out, respectively, to examine the effect. The conversion and MW were monitored by gas chromatography, gel permeation chromatography, and multiangle laser light scattering. The results suggested that CMS merely functioned as an initiator for St at the early stage; this led to linear macroinimers, which underwent SCATRP and gave rise to randomly branched polystyrene (PS) only at high conversion. The MI inimers formed charge-transfer complexes with St and underwent the SCATRP to result in hyperbranched copolymers at first; this initiated the atom transfer radical polymerization of St and led to star-shaped PS. With the objective of improving the processability and melt fluidity, the physical properties of poly(2,6-dimethyl-1,4-phenylene oxide) (PPO) blends with linear, randomly branched, and star-shaped PS were compared. In comparison with those with linear PS, the PPO/branched PS blends exhibited a higher glass-transition temperature, a higher melt flow index, and a comparable thermal stability because of the spherical architecture of the branched PS. J Appl Polym Sci 121: 2957–2968, 2011

Key words: atom transfer radical polymerization (ATRP); blends; branched; polystyrene; poly(phenylene oxide)

INTRODUCTION

Dendritic polymers, including dendrimers and hyperbranched polymers, represent a family of branched polymers with a spherical conformation, less chain entanglement, low melt viscosity, and so on. Dendrimers are perfectly symmetrical macromolecules typically prepared via a repeated condensation–deprotection process. On the other hand, hyperbranched polymers are obtained via a one-pot synthetic methodology, which gives rise to structurally less perfect counterparts with comparable properties.[1–5] Thus, there have been reports on the industrial production of hyperbranched poly(ethylene imine)s by BASF via the multibranching ring-opening polymerization of aziridine[6–9] and polyesters by Perstorp via the classical $A_2 + B_3$ polycondensation.[10–13] However, such methods are only applicable to a very limited number of specialty monomers.

Fréchet et al.[14] proposed the self-condensing vinyl polymerization (SCVP) of inimers to prepare hyperbranched polymers. Thereafter, extensive studies have been undertaken to obtain via SCVP hyperbranched polymers, especially polystyrenes (PSs), with a large variety of chemical compositions, topology, and functionalities. For example, Matyjaszewski, Wooley, and coworkers[15–17] performed the self-condensing atom transfer radical polymerization (SCATRP) of 4-chloromethylstyrene (CMS); this led to hyperbranched PS. Heidenreich and Puskas[18] explored thermally initiated reversible addition–fragmentation chain transfer polymerization using 4-vinylbenzyldithiobenzoate as an inimer-type chain-transfer agent. Tao et al.[19] tailor-designed a styrene (St)-based inimer containing a 2,2,6,6-tetramethyl-1-piperidinyloxy moiety, which underwent the

Additional Supporting Information may be found in the online version of this article.

Correspondence to: G. Zhai (zhai_gq@cczu.edu.cn).

Contract grant sponsor: Natural Science Foundation of China; contract grant number: 20674033.
Contract grant sponsor: Natural Science Foundation of Jiangsu Province; contract grant number: BK2008142.
Contract grant sponsor: Scientific Research Foundation for the Returned Overseas Chinese Scholars (State Education Ministry).

nitroxide-mediated radical polymerization and led to hyperbranched PS. Although the hyperbranched topology was clearly confirmed, there was no evidence on how the branched structure evolved in these reports.

Because of the nonhomopolymerizable character, the SCATRP of maleimide (MI)-type inimers, such as *N*-[4-(α-bromobutyryloxy)]phenyl maleimide, were reported to form linear polymers.[20] Thus, the self-condensing atom transfer radical copolymerization (SCATRcP) of MI inimers with a large excess of St have generally been explored,[20–22] and it has been claimed that because of the formation of charge-transfer complexes (CTCs) between MIs and St, SCATRcP led to hyperbranched copolymers at first. After the virtual depletion of the CTCs, the hyperbranched copolymers initiated the atom transfer radical polymerization (ATRP) of St and resulted in star-shaped PS.[20–22] Because of the difficulty in estimating the degree of branching, the ratio between the absolute weight-average molecular weight determined by multiangle laser light scattering ($M_{w.\mathrm{MALLS}}$) and the relative one determined by gel permeation chromatography ($M_{w.\mathrm{GPC}}$), or the $M_{w.\mathrm{MALLS}}/M_{w.\mathrm{GPC}}$ ratio, was used to verify the branched structure because it is widely accepted that the $M_{w.\mathrm{GPC}}$ of branched polymers is significantly lower than the corresponding $M_{w.\mathrm{MALLS}}$.[23] Our recent study[24] of the SCATRP of an MI-type inimer with St confirmed that the $M_{w.\mathrm{GPC}}/M_{w.\mathrm{MALLS}}$ ratio decreased gradually when the St conversion increased with the reaction time.

Because of their numerous graft chains and terminal functionalities, hyperbranched polymers have characteristics of less crystallinity, lower melt or solution viscosity, and lower mechanical strength. Recently, Jiang and coworkers[25–27] used hyperbranched PS as the viscosity modifier to blend with engineering plastics, such as polycarbonates, acrynitrile–butadiene–St copolymer, and nylon. After it was blended with hyperbranched PS, compared to pristine plastics, the alloy showed a much lower melt viscosity, whereas the thermal stability and mechanical properties remained almost constant.

Since its invention by Hay in 1954[28] and its commercial production by GE in 1962, poly(2,6-dimethyl-1,4-phenylene oxide) (PPO) has attracted much attention for its excellent chemical inertness, thermal stability, and mechanical properties.[29] However, because of its rigid backbone, PPO is also characterized by a high glass-transition temperature (T_g), a very low melt flow index (MFI), and a very high melt viscosity; this makes its melt processing highly energy-consuming. Thus, most commercially available PPOs are in the form of blends with styrenic polymers (e.g., Noryl resins of GE Plastics),[30–34] polyamides,[35] and polyesters.[36] Puskas et al.[30] investigated the thermal and rheological properties of blends of PPO with different thermoplastics, that is, PS-*b*-polyisobutylene-*b*-PS, PS-*b*-polybutadiene-*b*-PS, and PS-*b*-poly(ethylene/butylene)-*b*-PS. They observed that pronounced phase separation can occur. However, there has not yet been any report on PPO blends with branched styrenic polymers.

In this study, we compared the SCATRP of CMS and MI-type inimers with St, respectively, with an objective of experimentally investigating the effects of the reactivity ratios on the development of the branched structure and the architecture of the final polymers. Second, we tentatively blended linear and branched PSs with PPO and compared the thermal properties, such as the glass transition and thermal stability, of these blends. The study of the mechanical properties, such as the tensile and impact strengths, of the blends is still in progress at the time of this writing.

EXPERIMENTAL

Materials

CMS was from Wujin Linchuan Chemical Co., Ltd. (Changzhou, China). St, purchased from Shanghai Chemical Corp., Ltd. (Shanghai, China), was washed with a 10% aqueous solution of NaOH (100 mL) three times to remove the inhibitor, dried with $CaCl_2$ 24 h after it was washed with water, filtered, and distilled under reduced pressure. CuBr, also from Shanghai Chemical Corp., was purified by stirring in glacial acetic acid, washed with ethanol, and then dried *in vacuo* at 60°C. Pentamethyldiethylenetriamine (PMDETA) was from Liyang Jiangdian Fine Chemicals (Changzhou, China). PPO (LXR045) was purchased from Bluestar New Chemical Materials Co., Ltd. (Ruicheng, China). Linear general-purpose polystyrene (GPPS, PG-33) was from ChiMei Corp. (Zhenjiang, China). These compounds were used as received unless specified clearly.

Synthesis of the MI inimers

The synthetic route to the MI inimers is shown in Scheme 1. *N*-(4-Hydroxyl)phenyl maleimide (HPM) was prepared as reported elsewhere.[20,22] The purity was determined by high-performance liquid chromatography (HPLC) to be 99.84%. For the preparation of *N*-[4-(α-bromoisobutyryloxy)]phenyl maleimide (BiBPM), HPM (25.30 g, 0.13 mol), triethylamine (20.20 g, 0.20 mol), a small quantity of $CuCl_2$ (ca. 0.5–1 mol % to HPM), and dimethylformamide (80 mL) were added to a three-necked flask. The mixture was stirred until HPM was completely dissolved. Then, a mixture of α-bromoisobutyric acid chloride (32.30 g, 0.17 mol) and dimethylformamide (80 mL) was added dropwise to the flask with mild stirring. After a 4-h reaction at 40°C, the mixture

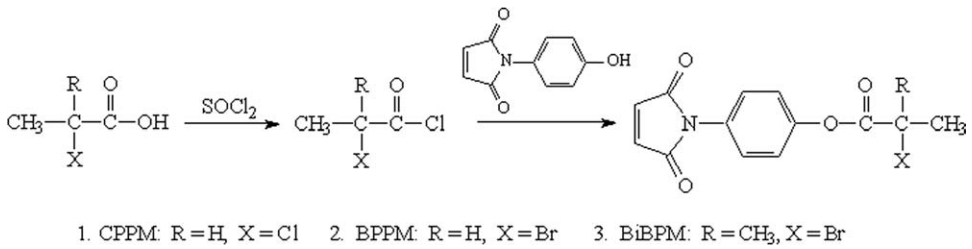

Scheme 1 Synthetic route to the MI inimers.

was poured into the ice water (2 L). BiBPM precipitated out from the water gradually and was collected by filtration and washed three times with copious amounts of water. The raw product was recrystallized from ethanol and was a brown powder. The yield was 50–55%. *N*-[4-(α-Chloropropionyloxy)]phenyl maleimide (CPPM) and *N*-[4-(α-bromopropionyloxy)]phenyl maleimide (BPPM) were prepared and recrystallized with a similar protocol to that used for BiBPM. They were obtained in the form of slightly yellow needlelike crystals. The corresponding yield was about 50–60%.

SCATRP of CMS with St

The SCATRP of CMS with St was carried out as follows: CMS (0.31 g, 0.002 mol), St (10.41 g, 0.10 mol), CuBr (0.29 g, 0.002 mol), PMDETA (1.04 g, 0.006 mol), and a magnetic bar were added to a 100-mL flask. The mixture was cycled between vacuum and argon five times, after which the mixture was sealed and left to react in an oil bath at 120°C with mild stirring. The aliquots were withdrawn from the reaction mixture for NMR and gel permeation chromatography (GPC) measurement. After the reaction, the flask was allowed to cool to room temperature, and 50 mL of tetrahydrofuran (THF) was added to dilute the mixture. The mixture was precipitated into ethanol (0.80 L). The resulting PS was obtained by filtration and dried at 45°C for 24 h. The St conversion was calculated by ^{1}H-NMR spectroscopy. The experimental details are listed in Table I.

TABLE I
Experimental Details of the SCATRP of St- and MI-Type Inimers with St

Experiment	Inimer	[Inimer]:[St]:[CuBr]:[PMDETA][a]	Temperature (°C)
1	CMS	2 : 200 : 2 : 6	120
2	CPPM	4 : 200 : 2 : 6	80
3	BPPM	4 : 200 : 2 : 6	80
4	BiBPM	4 : 200 : 1 : 3	80

[a] The volume of St was fixed at 50 mL, and no solvent was used.

SCATRP of MI-type inimers with St

For a typical experiment, BiBPM (1.35 g, 0.004 mol), St (10.41 g, 0.1 mol), CuBr (0.14 g, 0.001 mol), PMDETA (0.52 g, 0.003 mol), and a magnetic bar were added to a 100-mL flask. The mixture was cycled between vacuum and argon five times, after which the mixture was sealed and left to react in a water bath at 80°C. Other procedures were similar to the those mentioned previously. The experimental details are also listed in Table I.

NMR spectroscopy

The ^{1}H-NMR spectroscopy was recorded on a Bruker ARX-500 NMR spectrometer (Zurich, Switzerland) at room temperature in $CDCl_3$..

GPC–multiangle laser light scattering (MALLS)

The apparent number-average and weight-average molecular weights determined by gel permeation chromatography ($M_{n,GPC}$ and $M_{w,GPC}$, respectively) and molecular weight distribution (MWD) were determined on a GPC setup consisting of a Waters 1515 isocratic pump, Waters Styragel HR 4e, HR 1 and HR 0.5 columns, a Waters 2414 refractive-index detector, and a Waters 717 autosampler (Milford, Massachusetts). The eluent was THF at a flow rate of 1 mL/min at 35°C. The apparent molecular weight (MW) was calibrated against linear PS standards and generated from Waters Breeze software. The absolute weight-average molecular weight determined by multiangle laser light scattering ($M_{w,MALLS}$) was determined by a Wyatt miniDAWN Tri-Star MALLS detector (Santa Barbara, California), and the data were treated with Wyatt ASTRA software. The differential refractive-index increment of PS in THF was fixed at 0.185 mL/g..

Blending of PPO and PS with an internal mixer

The blending of PPO with PS was carried out on an Su-70 internal mixer (Suyan Technology, Changzhou, China). The PS samples used are shown in Table II. Predetermined amounts of PPO and PS, the total weight of which was fixed at about 50 g, were added

TABLE II
PS Samples Used to Blend with PPO

Sample entry	Inimer	$M_{n,GPC}$	$M_{w,GPC}$	$M_{w,GPC}/M_{n,GPC}$	$M_{w,MALLS}$	$M_{w,MALLS}/M_{w,GPC}$	T_g (°C)
PS_0 (GPPS)	Not applicable	1.18×10^5	2.11×10^5	1.79	2.59×10^5	1.23	97.91
PS_1	CPPM	2.72×10^4	8.25×10^4	3.03	1.99×10^5	2.41	92.36
PS_2	BPPM	2.73×10^4	1.27×10^5	4.65	2.79×10^5	2.20	93.67
PS_3	BiBPM	3.13×10^4	1.10×10^5	3.51	3.54×10^5	3.22	107.06
PS_4	CMS	3.94×10^4	1.36×10^5	3.45	4.73×10^5	3.48	101.22

to the cylinder, sealed, heated to 280°C, and mixed at 30 Hz for 8 min. After it was cooled to room temperature, the blend was removed from the cylinder for subsequent measurement. PPO/PS_0 (90 : 10) denoted the blend that contained 45 g of PPO and 5 g of PS_0, where 90 and 10 represented the weight percentage of PPO and PS0 in the blend.

Differential scanning calorimetry (DSC)

The T_g values of the PPO/PS blends were determined on a PerkinElmer Pyris-1 differential scanning calorimeter (Waltham, Massachusetts). Each sample was heated from 40 to 250°C under an N_2 atmosphere at a heating rate of 20°C/min, after which the sample was cooled rapidly to room temperature and then heated to 250°C at the same rate. The second cycle was recorded for the T_g measurement.

Thermogravimetric analysis (TGA)

The thermal stability of the PPO/PS blend was evaluated on a SDT Q600 thermogravimetric analyzer (TA Instruments, Twin Lakes, Wisconsin) under an N_2 atmosphere at a heating rate of 10°C/min.

Determination of MFI

The MFI of the PPO/PS blends was measured on a MFI tester (SANS, Shenzhen, China) under a load of 5 kg at 280°C. The preheating time was 5 min. Each experiment was repeated five times, and the average value was noted as the MFI.

RESULTS AND DISCUSSION

Preparation of the MI inimers

The intermediate, HPM, was prepared as reported elsewhere.[20,22,24] The inimers, CPPM, BPPM, and BiBPM, were prepared via the esterification of HPM with the corresponding carboxylic acid chloride, as illustrated in Scheme 1. Figures 1–3 show the ^{1}H-NMR spectra and peak assignments of CPPM, BPPM, and BiBPM, respectively. For CPPM and BPPM, the peaks at δ = 7.2–7.5, 6.9, and 4.5–4.7 ppm were assigned to the aromatic protons (Ar—*H*), the MI protons (—C*H*=C*H*—), and the proton adjacent to the ester moiety (—OCOC*H*—). The [—OCOC*H*—]:[—C*H*=]:[—C_6H_4—] molar ratios were estimated from the corresponding spectral integrals to be about 1 : 1.98 : 4.33 and 1 : 1.90 : 3.85, respectively; these values were in good agreement with the stoichiometric ratio. For BiBPM, the peaks at δ = 7.2–7.5, 6.9, and 2.1 ppm were assigned to the Ar—*H*, —C*H*=C*H*—, and —CH_3 moieties, respectively. The [Ar—*H*]:[—C*H*=C*H*—]:[—CH_3] molar ratio, determined from the spectral integrals, was about 2 : 1 : 2.74; this was in moderate agreement with the theoretical value. Additionally, the purity

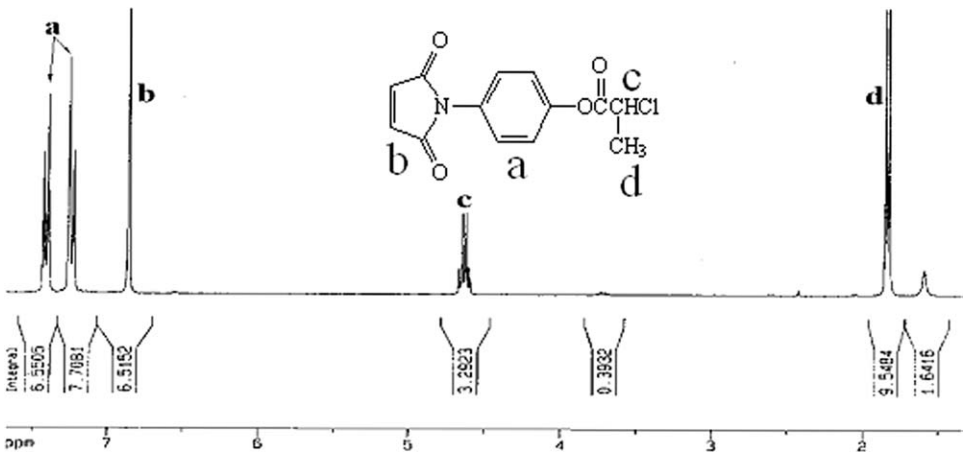

Figure 1 ^{1}H-NMR spectrum of the inimer CPPM with $CDCl_3$ as the solvent.

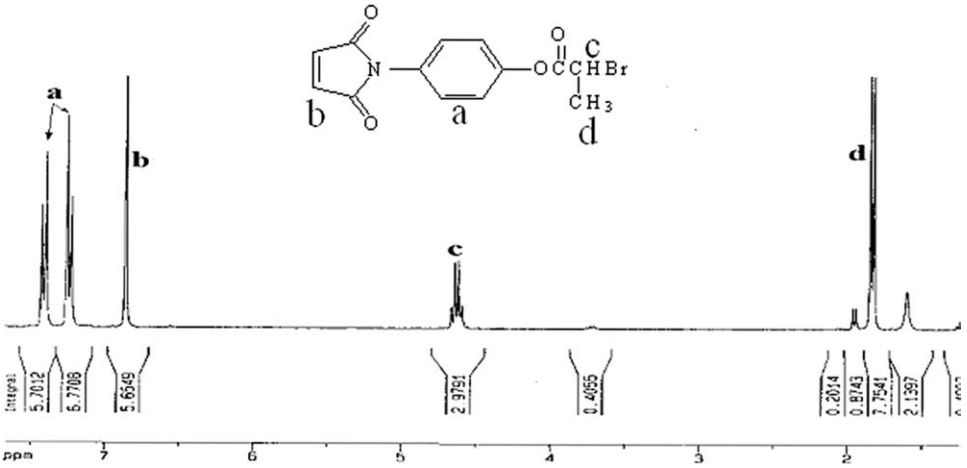

Figure 2 ^{1}H-NMR spectrum of the inimer BPPM with $CDCl_3$ as the solvent.

was determined by HPLC to be above 98%. Thus, these results confirmed that the inimers thus prepared had good purity for the subsequent SCATRcP.

SCATRP of CMS with St

Figure 4(a) shows the kinetic plots of the SCATRP of CMS with St. The reaction temperature for experiment 1 should have been well above 100°C because of the low initiating ability of the benzylic chloride moiety.[23,37] Figure 4(b) shows the semilogarithmic plot of experiment 1. It appeared that the SCATRP of CMS with St proceeded in a well-controlled fashion; that is, the concentration of the propagating radicals remained almost constant because the plot was approximately linear. The apparent propagation rate constant of experiment 1, as derived from the fitted slope, was about 9.40×10^{-5} s^{-1}.

Figure 5(a) shows the GPC chromatograms of the PS samples taken from experiment 1 at different conversions. PS maintained a narrow MWD at low conversion. However, it became gradually broader as the reaction proceeded. Furthermore, as observed from the GPC chromatograms, diametrically opposite to the monomodal distribution of the those at low conversion, the PS samples collected at high conversion exhibited a typical multimodal distribution.

Figure 5(b) shows the $M_{n,GPC}$, $M_{w,GPC}$, MWD ($M_{w,GPC}/M_{n,GPC}$), and branching frequency (BR) of the PSs obtained in experiment 1 at different conversions. BR was estimated from the conversion and GPC data with the following equation[38]:

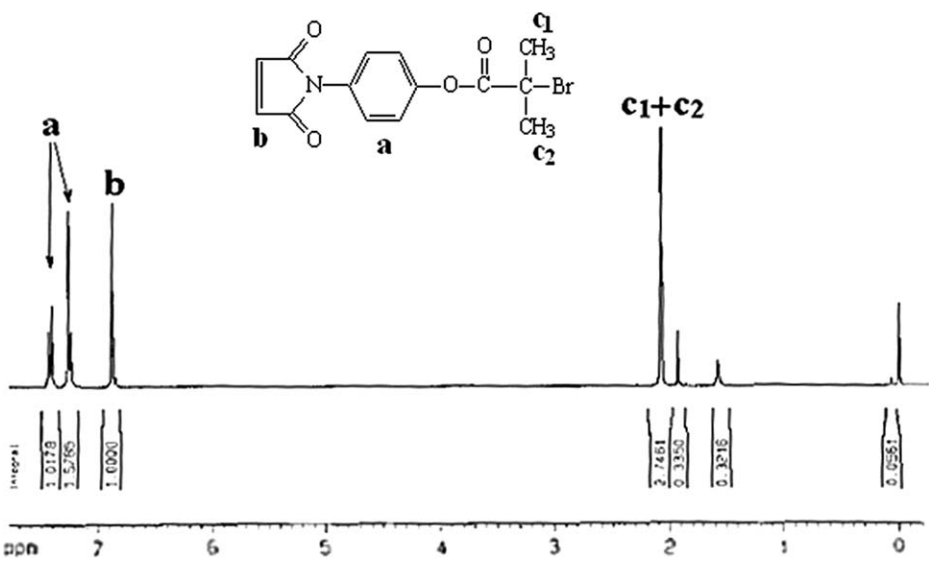

Figure 3 ^{1}H-NMR spectrum of the inimer BiBPM with $CDCl_3$ as the solvent.

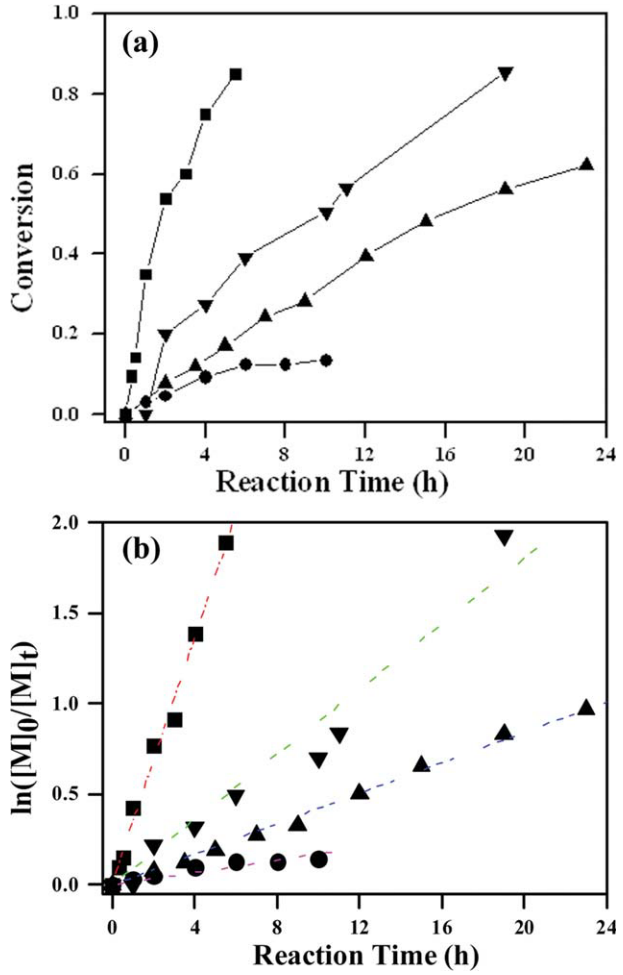

Figure 4 (a) Time–conversion profiles of experiments (■) 1, (●) 2, (▲) 3, and (▼) 4. Experiment 1 : [CMS] : [St] : [CuBr]: [PMDETA] = 2 : 200 : 2 : 6 at 120°C. Experiment 2: [CPPM] : [St] : [CuBr] : [PMDETA] = 4 : 200 : 2 : 6 at 80°C. Experiment 3 : [BPPM] : [St] : [CuBr] : [PMDETA] = 4 : 200 : 2 : 6 at 80°C. Experiment 4 : [BiBPM] : [St] : [CuBr] : [PMDETA] = 4 : 200 : 1 : 3 at 80°C. (b) Semilogarithmic plots of experiments (■) 1, (●) 2, (▲) 3, and (▼) 4. Experiment 1 : [CMS] : [St]: [CuBr] : [PMDETA] = 2 : 200 : 2 : 6 at 120°C. Experiment 2 : [CPPM] : [St] : [CuBr] : [PMDETA] = 4 : 200 : 2 : 6 at 80°C. Experiment 3 : [BPPM] : [St] : [CuBr] : [PMDETA] = 4 : 200 : 2: 6 at 80°C. Experiment 4 : [BiBPM] : [St] : [CuBr] : [PMDETA] = 4 : 200 : 1 : 3 at 80°C. [M]0 and [M]t were the initial monomer concentration and the monomer concentration at the moment t. [Color figure can be viewed in the online issue, which is available at wileyonlinelibrary.com.]

$$\mathrm{BR} = \frac{M_{n,\mathrm{GPC}}}{M_{n,\mathrm{theo}}} - 1 = \frac{M_{n,\mathrm{GPC}}}{\frac{[\mathrm{St}]_0}{[\mathrm{Inimer}]_0} \times \mathrm{Conversion} \times 104} - 1 \quad (1)$$

The results show that the PS had a narrow MWD and low BR (<1) when the conversion was less than 0.5. This indicated that there was almost no branched structure formed at this stage. However, when the conversion was over 0.5, MWD and, especially, BR increased very remarkably. For example, BR increased from 0.6 to 1.6, 2.5, and 4.2 when the conversion grew from 0.52 to 0.60, 0.75, and 0.85, respectively. In other words, there were about six chains per PS macromolecule when the conversion was above 0.80. The results suggest that the SCATRP of CMS with St could be treated as a two-phase process. Because $r_1 \approx r_2 \approx 1$ (where r_1 is the reactivity ratio of CMS and r_2 is the reactivity ratio of St) and because there was a very low concentration, CMS functioned as an initiator at the early stage and led to linear PS macroinimers. After the St conversion was rather high (well above 0.5), the macroinimer underwent SCATRP and formed a randomly branched PS. This process is schematically illustrated in Scheme 2.

Such a concept was also supported by the MALLS data. Figure 6 shows the $M_{w,\mathrm{GPC}}$, $M_{w,\mathrm{MALLS}}$, and $M_{w,\mathrm{MALLS}}/M_{w,\mathrm{GPC}}$ ratio of the PS from experiment 1. On the one hand, both $M_{w,\mathrm{GPC}}$ and $M_{w,\mathrm{MALLS}}$ increased steadily with conversion; on the other

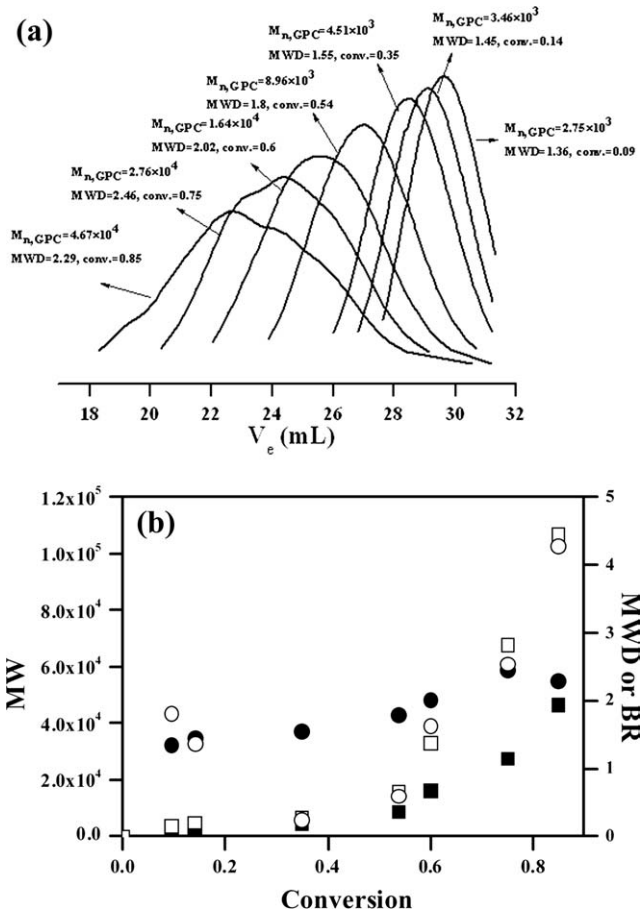

Figure 5 (a) GPC chromatograms of the PS prepared from experiment 1 at different conversions (conv.'s). Experiment 1 : [CMS] : [St] : [CuBr] : [PMDETA] = 2 : 200 : 2 : 6 at 120°C. (b) (■) $M_{n,\mathrm{GPC}}$, (□) $M_{w,\mathrm{GPC}}$, (●) MWD, and (○) BR of the PS prepared from experiment 1 at different conversions. Experiment 1 : [CMS] : [St] : [CuBr] : [PMDETA] = 2 : 200 : 2 : 6 at 120°C.

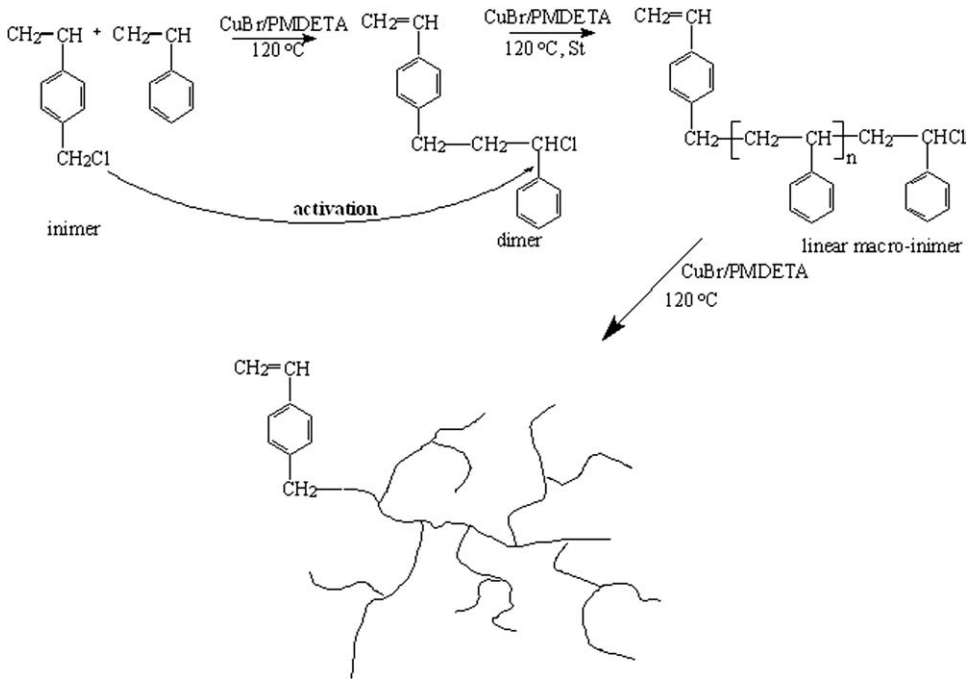

Scheme 2 SCATRP of CMS with St.

hand, the $M_{w,\mathrm{MALLS}}/M_{w,\mathrm{GPC}}$ ratio also increased significantly with conversion, especially when the conversion was above 0.5. The results also confirm that the branched architecture was formed only at high conversion in the SCATRP of CMS with St.

SCATRP of the MI inimers with St

The alternating ATRP of electron-rich monomers (e.g., vinylic aromatics, dienes) and electron-deficient monomers (e.g., maleic anhydride, MIs) has been investigated.[39–43] Yan, Liu, and coworkers[44,45] also reported on SCVP of donor–acceptor pairs, which resulted in hyperbranched copolymers.

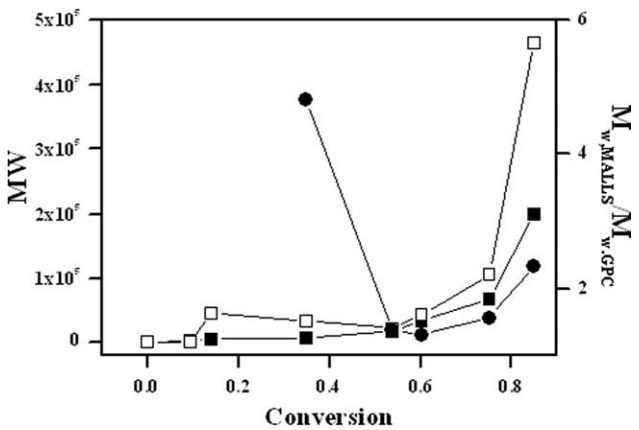

Figure 6 (■) $M_{w,\mathrm{GPC}}$, (□) $M_{w,\mathrm{MALLS}}$, and (●) $M_{w,\mathrm{MALLS}}/M_{w,\mathrm{GPC}}$ ratio of the PS prepared from experiment 1 at different conversions. Experiment 1 : [CMS] : [St] : [CuBr] : [PMDETA] = 2 : 200 : 2 : 6 at 120°C.

The kinetic plots of experiments 2–4 are also shown in Figure 4(a). Their reaction temperature was fixed at 80°C because 2-chloropropionyloxy, 2-bromopropionyloxy, and α-bromoisobutyryloxy were reported to have a much higher initiating activities than benzyl chloride.[46] It was obvious that the conversion increased gradually with the reaction time. Figure 2(a) also shows that the reaction rate of the SCATRP of the MI inimers with St ascended in the following order: CPPM < BPPM < BiBPM. This order was attributed to the initiation activity in the order 2-Chloropropionyloxy < 2-Bromopropionyloxy < α-Bromoisobutyryloxy.[46] The semilogarithmic plots of experiments 2–4 are also shown in Figure 4(b). The corresponding apparent propagation rate constants were estimated to be about 4.72×10^{-6}, 1.17×10^{-5}, and 2.50×10^{-5} s^{-1}, respectively. As also shown in Figure 4(a), the kinetic plot for experiment 2 leveled much faster than those for experiments 1, 3, and 4. This was probably due to the deactivation of the growing chains with aliphatic amines, such as PMDETA.[47–49]

Figure 7(a) shows the GPC chromatograms of PS from experiment 4 at different conversions. The GPC chromatograms showed that the PS at the low conversion had a lower and monomodal MWD. However, with increasing conversion, a shoulder peak appeared at the high-MW side, as we[24] and Deng and Chen[21] noted previously. This was attributed to the bimolecular termination of the propagating radicals because the MW seemed double that of the main peak.[18,24,50] Figure 7(b) shows $M_{n,\mathrm{GPC}}$, $M_{w,\mathrm{GPC}}$, MWD, and BR for experiment 4. Both MW and

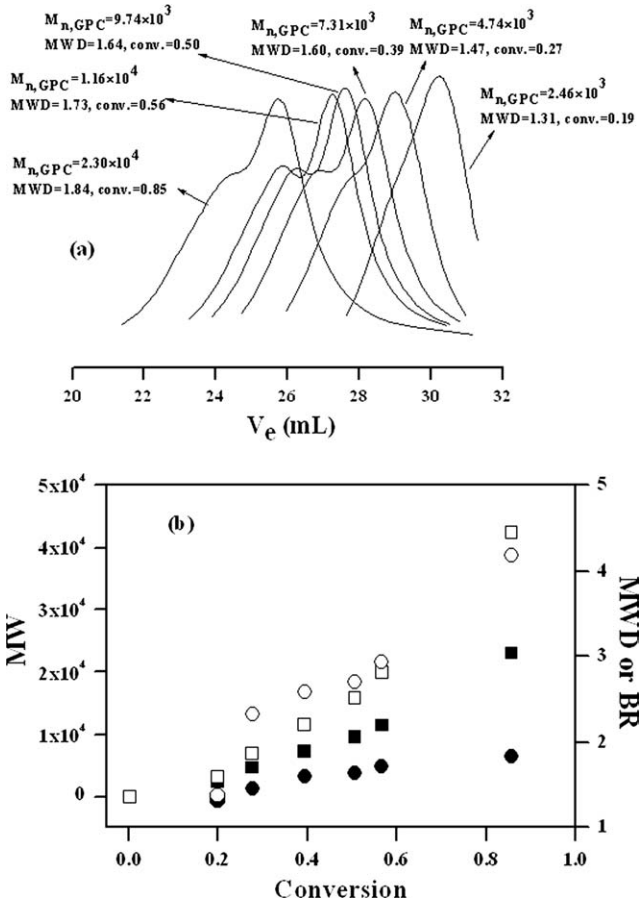

Figure 7 (a) GPC chromatograms of the PS prepared from experiment 4 at different conversions. Experiment 4 : [BiBPM] : [St] : [CuBr] : [PMDETA] = 4 : 200 : 1 : 3 at 80°C. (b) (■) $M_{n,GPC}$, (□) $M_{w,GPC}$, (●) MWD, and (○) BR of the PS prepared from experiment 4 at different conversions. Experiment 4 : [BiBPM] : [St] : [CuBr] : [PMDETA] = 4 : 200 : 1 : 3 at 80°C.

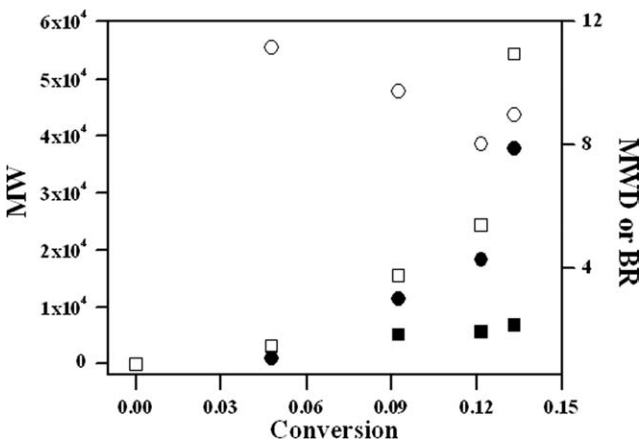

Figure 8 (■) $M_{n,GPC}$, (□) $M_{w,GPC}$, (●) MWD, and (○) BR of the PS prepared from experiment 2 at different conversions. Experiment 2 : [CPPM] : [St] : [CuBr] : [PMDETA] =4 : 200 : 2 : 6 at 80°C.

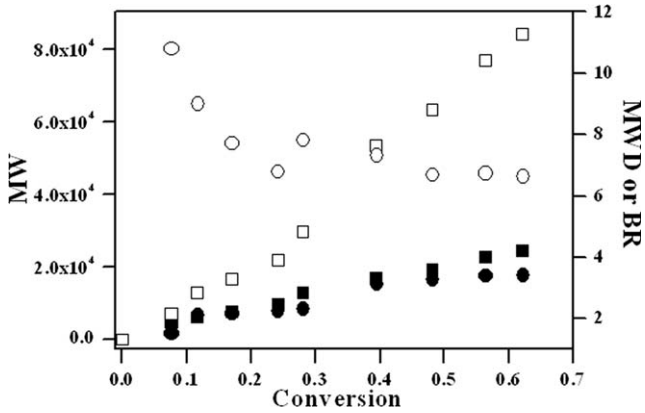

Figure 9 (■) $M_{n,GPC}$, (□) $M_{w,GPC}$, (●) MWD, and (○) BR of the PS prepared from experiment 3 at different conversion. Experiment 3 : [BPPM] : [St] : [CuBr] : [PMDETA] = 4 : 200 : 2 : 6 at 80°C.

MWD increased gradually with the conversion. However, BR also grew steadily, especially when the conversion was above 0.5. On the basis of the GPC chromatograms, this was primarily attributed to the bimolecular termination.

Figures 8 and 9 also show $M_{n,GPC}$, $M_{w,GPC}$, MWD, and BR of the St–MI copolymer prepared from experiments 2 and 3 at different conversions, respectively. In common and similar to that of experiment 4, both $M_{n,GPC}$ and $M_{w,GPC}$ increased gradually with the conversion. The PS prepared from experiments 2 and 3 had a much larger MWD than those from experiment 4 at comparable conversions. Close comparison revealed that MWD of the St–MI copolymer prepared from experiments 2–4 were in the following order: Experiment 4 < Experiment 3 < Experiment 2. This was contrary to the initiation activity of the inimers used. Thus, such results indicated that an inimer of higher initiation activity could give rise to a narrower MWD.

The BR data from experiments 2 and 3 suggested that in contrast to experiment 4, BR underwent a slight decrease at first and then remained almost constant with the conversion. Because CPPM and BPPM exhibited a much lower initiation activity than BiBPM, the concentration of the propagating radicals of the previous experiments were in the order: CPPM < BPPM < BiBPM, as shown in Figure 4. The bimolecular termination was negligible in experiments 2 and 3. Therefore, these results implied that the number of PS chains per PS macromolecule was maintained at about 9 and 7 for experiments 2 and 3, respectively. We admit that polymers obtained by radical–radical combination may misinterpret the branching efficiency.

Figures 10–12 show the $M_{w,GPC}$, $M_{w,MALLS}$, and $M_{w,MALLS}/M_{w,GPC}$ ratio of the PS from experiments

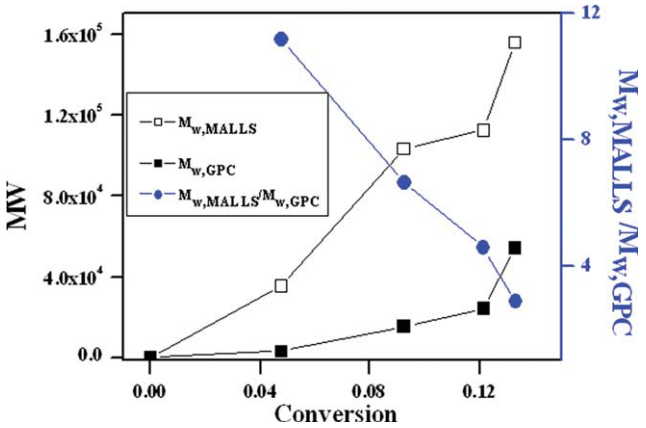

Figure 10 (■) $M_{w,GPC}$, (□) $M_{w,MALLS}$, and (●) $M_{w,MALLS}/M_{w,GPC}$ ratio of the PS obtained in experiment 2 at different conversions. Experiment 2: [CPPM] : [St] : [CuBr] : [PMDETA] = 4 : 200 : 2 : 6 at 80°C. [Color figure can be viewed in the online issue, which is available at wileyonlinelibrary.com.]

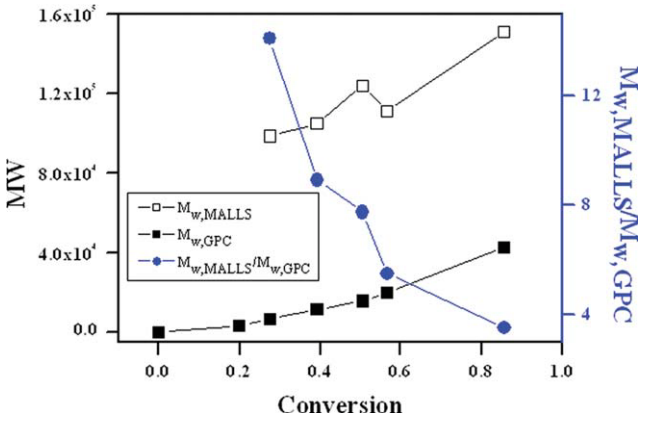

Figure 12 (■) $M_{w,GPC}$, (□) $M_{w,MALLS}$, and (●) $M_{w,MALLS}/M_{w,GPC}$ ratio of the PS obtained in experiment 4 at different conversions. Experiment 4: [BiBPM] : [St] : [CuBr] : [PMDETA] = 4 : 200 : 1 : 3 at 80°C. [Color figure can be viewed in the online issue, which is available at wileyonlinelibrary.com.]

2–4 at different conversions. It was clear that the $M_{w,MALLS}/M_{w,GPC}$ ratio was rather high initially. In particular, the $M_{w,MALLS}/M_{w,GPC}$ ratios were about 11, 7, and 14 when the conversions were about 0.05, 0.07, and 0.27 for the PSs prepared from experiments 2, 3, and 4, respectively. Such ratios implied that the PS at low conversion was hyperbranched. However, the $M_{w,MALLS}/M_{w,GPC}$ ratio underwent a gradual decrease with the conversion in a diametrically opposite fashion to the SCATRP of CMS with St (see Fig. 6). Thus, the SCATRcP of the MI inimers with a large excess of St was composed of two different phases, both mechanistically and kinetically. Because $r_1 \approx r_2$ (where r_1 is the reactivity ratio of the MI inimers and r_2 is the reactivity ratio of St) ≈ 0, they formed an inimer-type CTC with a much greater reactivity;[51] this was preferentially polymerized into hyperbranched alternating copolymers via SCATRcP. It came to an end when the CTC was virtually depleted. Subsequently, the hyperbranched copolymers initiated the ATRP of St in a core-first fashion and led to star-shaped PS, as shown in Scheme 3. After the formation of the branched core, the further ATRP of St predominantly led to an increase in the linear St units, and, thus, the $M_{w,MALLS}/M_{w,GPC}$ ratio decreased with the conversion.

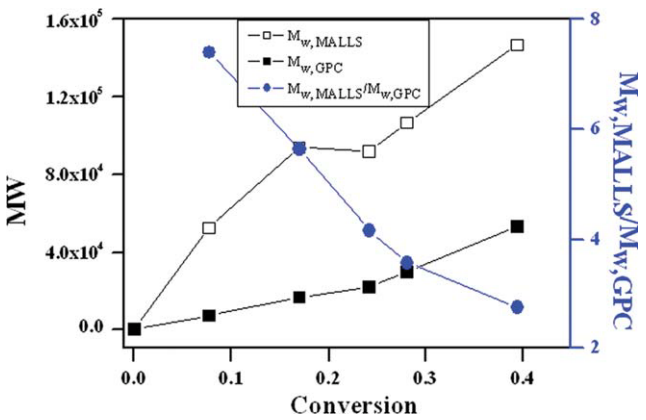

Figure 11 (■) $M_{w,GPC}$, (□) $M_{w,MALLS}$, and (●) $M_{w,MALLS}/M_{w,GPC}$ ratio of the PS obtained in experiment 3 at different conversions. Experiment 3: [BPPM] : [St] : [CuBr] : [PMDETA] = 4 : 200 : 2 : 6 at 80°C. [Color figure can be viewed in the online issue, which is available at wileyonlinelibrary.com.]

Physical properties of the PPO/branched PS blends

Four PS samples were prepared from experiments 1–4; their MWs are listed in Table II. Additionally, the commercially available linear GPPS was also used to prepared blends with PPO. After the preparation of the PPO/PS blends, the melt and thermal properties of the blends were compared.

Figure 13 shows the DSC thermograms of the PPO/PS_4 blends. The pristine PPO exhibited a T_g of about 221°C. After PPO was blended with PS_4 at a weight ratio of 90 : 10, the blend showed a T_g of 217°C. Further increases in the PS_4 content to 80 : 20 and 70 : 30 led to a lower T_g at 185 and 174°C, respectively. The DSC thermograms in Figure 8(a) also show that molecular compatibility was achieved between PPO and PS because only one glass transition was observed, even at higher PS contents.

Figure 14 shows the dependence of T_g of the PPO/PS blends with different PS samples on the PS content. The addition of linear GPPS led to a most significant decrease in T_g. For example, T_g of the PPO/PS_0 blends steadily decreased to 201, 184, and

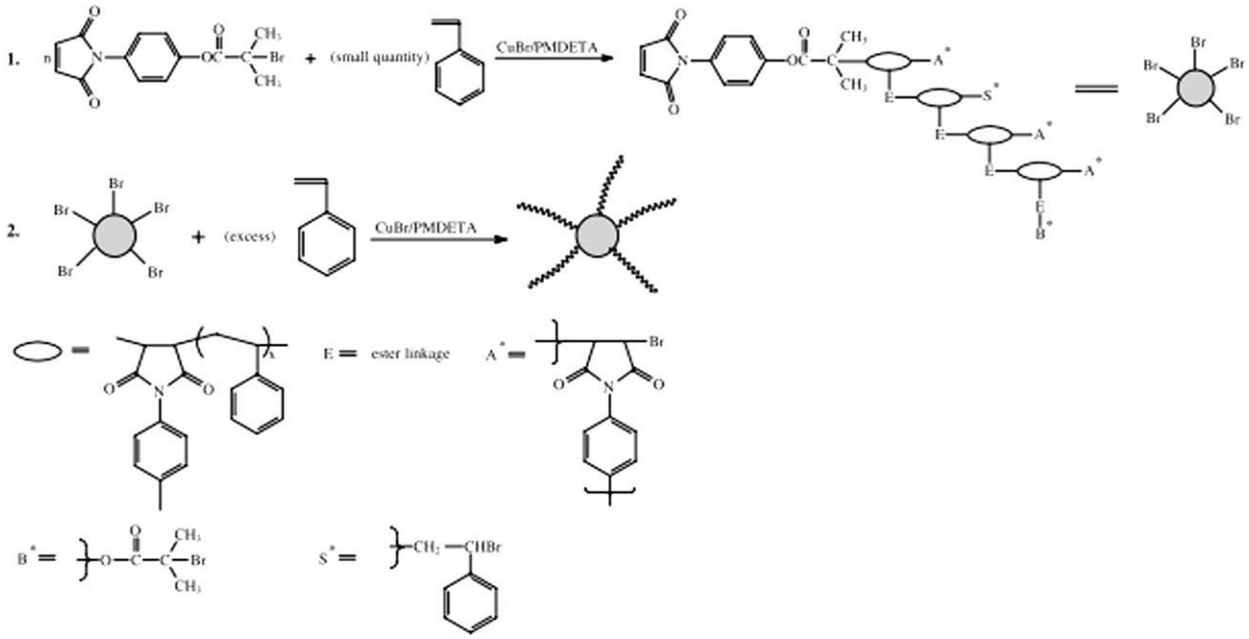

Scheme 3 SCATRP of the MI inimers with St.

168°C when the feed ratios were set at 90 : 10, 80 : 20, and 70 : 30, respectively. In comparison, the blends of PPO with randomly branched or star-shaped PS gave rise to a less obvious decrease in T_g. In other words, when blended with PPO, branched PS might have helped to maintain the mechanical strength at high temperature. Figure 14 also suggests that the Fox's law governing the T_g of the polymer blends might not have been applicable for systems in which at least one component is of branched topology. Also, our data implied that GPPS showed a comparable effect with PS-*b*-polyisobutylene-*b*-PS and PS-*b*-poly(ethylene/butylene)-*b*-PS in maintaining T_g of the blends, and branched PSs exhibited similar results to that of PS-*b*-polybutadiene-*b*-PS.[30]

Figure 15 shows the dependence of the MFI of the PPO/PS blends on the PS contents. The pristine PPO resin showed a very marginal fluidity at 280°C so that no melt flowed out, even for 10 min under 5 kg of pressure. The addition of GPPS to a feed ratio of as high as 70 : 30 showed little enhancement in MFI. On the other hand, the PPO blends with randomly branched or star-shaped PS exhibited much improved MFIs, especially PPO/PS_1 and PPO/PS_2; this was probably due to a lower $M_{n,GPC}$ of the branched PSs used.

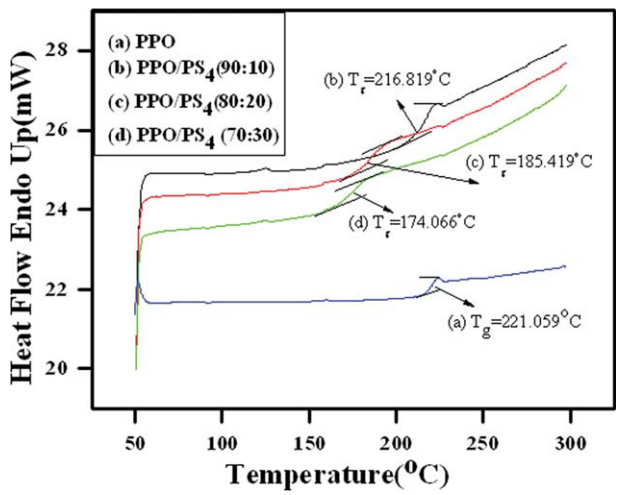

Figure 13 DSC thermograms of the PPO/PS4 blends at different weight feed ratios. [Color figure can be viewed in the online issue, which is available at wiley onlinelibrary.com.]

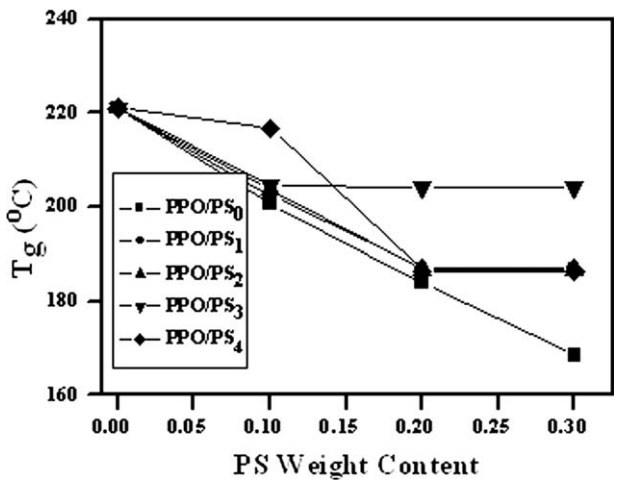

Figure 14 Dependence of T_g of the PPO/PS blends on the PS contents.

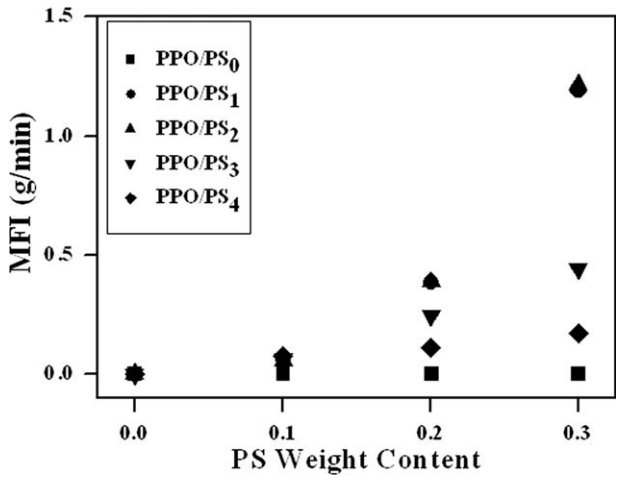

Figure 15 Dependence of MFI of the PPO/PS blends on the PS contents.

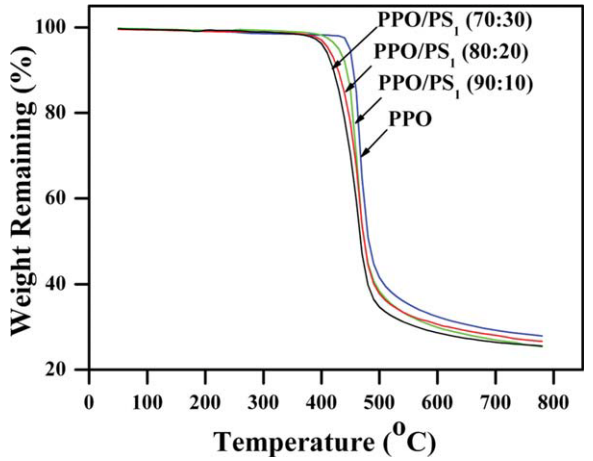

Figure 17 TGA curves of PPO/PS_1 at different weight feed ratios. [Color figure can be viewed in the online issue, which is available at wileyonlinelibrary.com.]

Figures 16 and 17 show the TGA curves of the PPO blends with the PS_0 and PS_1 samples, respectively, at different feed ratios (for the TGA curves of the PPO blends with other branched PS samples, see the Supporting Information). Clearly, a significant amount of residue was observed, especially for the blends of PPO with different PSs, and the residue increased gradually with increasing content of PS. On the other hand, the addition of PS into the PPO militated the thermal stability of PPO more or less. For the blends with feed ratios of 90 : 10 and 80 : 20, the PPO/PS_0 blends exhibited better thermal stabilities than the blends with branched PS samples; this was mainly ascribed to the C—Cl or C—Br terminal residues of the branched PS samples.[22,52,53] For example, when the feed ratio was fixed at 90 : 10, the values of 5% loss temperature, that is, the temperature at which the sample underwent a 5% weight loss, for the PPO/PS_0, PPO/PS_1, PPO/PS_2, PPO/PS_3, and PPO/PS_4 blends were about 440, 430, 430, 420, and 420°C, respectively. Furthermore, when the feed ratio was shifted to 80 : 20, the 5% loss temperatures for the PPO/PS_0, PPO/PS_1, PPO/PS_2, PPO/PS_3, and PPO/PS_4 blends were about 440, 410, 410, 410, and 410°C, respectively. However, with a feed ratio of 70 : 30, the blends exhibited comparable thermal stability. In particular, their 5% loss temperatures were about 410, 400, 400, 400, and 400°C, respectively. Thus, these results indicate that when the PS content was above 30%, GPPS exhibited no advantage over the branched PS, which contained thermally labile C—Cl or C—Br moieties.

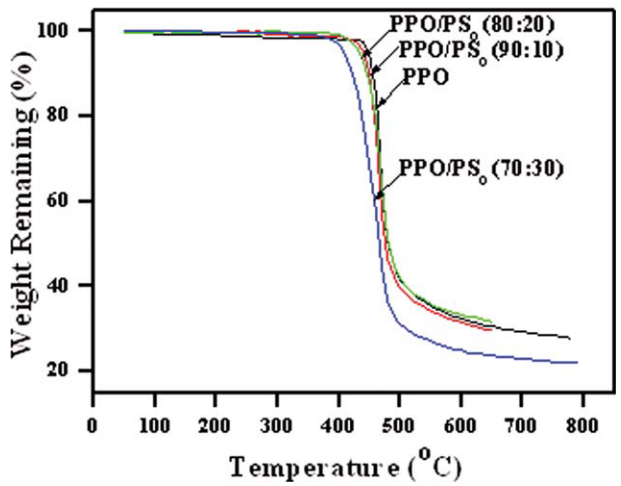

Figure 16 TGA curves of PPO/PS_0 at different weight feed ratios. [Color figure can be viewed in the online issue, which is available at wileyonlinelibrary.com.]

CONCLUSIONS

The effects of the reactivity ratio of the inimer and comonomer on the SCATRP kinetics and especially the evolution of branched structure were investigated. Also, the physical properties of the PPO/PS blends was correlated to the macromolecular architecture of PS. The SCATRP of CMS and MI inimers with a large excess of St was carried out. The kinetic study suggested that when $r_1 \approx r_2 \approx 1$, CMS functioned as a typical initiator initially at conditions of high St concentration, gave rise to linear macroinimers, which underwent the SCATRP, and led to randomly branched PS only at the high conversion. However, when $r_1 \approx r_2 \approx 0$, the MI inimers formed CTC with St, undergoing the SCATRP to result in the hyperbranched copolymer at the early stage, which initiated ATRP of St and led to star-shaped PS finally. Thus, SCATRP of the inimers with a large excess of comonomers produced randomly branched polymers and star-shaped polymers when $r_1 \approx r_2 \approx 1$

and $r_1 \approx r_2 \approx 0$, respectively. When PS was blended with PPO, both the randomly branched and star-shaped PS exhibited a superior advantage over GPPS in improving MFI and maintaining T_g of the alloys. However, because of the thermally labile C—Cl or C—Br moiety, the PPO/branched PS blends showed a lower thermal stability than the corresponding PPO/GPPS.

References

1. Hawker, C. J. Adv Polym Sci 1999, 147, 113.
2. Hult, A.; Johansson, M.; Malmström, E. Adv Polym Sci 1999, 143, 1.
3. Gao, C.; Yan, D. Y. Prog Polym Sci 2004, 29, 183.
4. Jikei, M.; Kakimoto, M. Prog Polym Sci 2001, 26, 1233.
5. Mori, H.; Müller, A. H. E. Top Curr Chem 2003, 228, 1.
6. Oxazogen, Inc.; Yin, R.; Tomalia, D. A.; Qin, D. J.; Dunham, J. A. PCT/U.S. Pat. 002838 (1998).
7. Pericet-Camara, R.; Papastavrou, G.; Behrens, S. H.; Helm, C. A.; Borkovec, M. J Colloid Interface Sci 2006, 296, 496.
8. Oulantia, O.; Pefferkorn, E.; Champ, S.; Auweter, H. J Colloid Interface Sci 2006, 296, 9.
9. Orlicki, J. A.; Kosik, W. E.; Demaree, J. D.; Bratcher, M. S.; Jensen, R. E.; McKnight, S. H. Polymer 2007, 48, 2818.
10. Sendijarevic, I.; McHugh, A. J. Macromolecules 2000, 33, 590.
11. Pruthtikul, R.; Coleman, M. M.; Painter, P. C.; Tan, N. P. J Polym Sci Part B: Polym Phys 2001, 39, 1651.
12. Fröhlich, J.; Kautz, H.; Thomann, R.; Frey, H.; Mülhaupt, R. Polymer 2004, 45, 2155.
13. Wang, J. R.; Xu, T. W. Polym Adv Technol [Online early access]. Published Online: 2009. DOI: 10.1002/pat.1544
14. Fréchet, J. M. J.; Henmi, M.; Gitsov, I.; Aoshima, S.; Leduc, M. R.; Grubbs, R. B. Science 1995, 269, 1080.
15. Gaynor, S. G.; Edelman, S.; Matyjaszewski, K. Macromolecules 1996, 29, 1079.
16. Powell, K. T.; Cheng, C.; Wooley, K. L. Macromolecules 2007, 40, 4509.
17. Cheng, C.; Wooley, K. L.; Khoshdel, E. J Polym Sci Part A: Polym Chem 2005, 43, 4754.
18. Heidenreich, A. J.; Puskas, J. E. J Polym Sci Part A: Polym Chem 2008, 46, 7621.
19. Tao, Y. F.; He, J. P.; Wang, Z. M.; Pan, J. Y.; Jiang, H. J.; Chen, S. M.; Yang, Y. L. Macromolecules 2001, 34, 4742.
20. Ren, Q.; Gong, F. H.; Jiang, B. B.; Zhang, D. L.; Fang, J. B.; Guo, F. D. Polymer 2006, 47, 3382.
21. Deng, G. H.; Chen, Y. M. Macromolecules 2004, 37, 18.
22. Ren, Q.; Jiang, B. B.; Zhang, D. L.; Yu, Q.; Fang, J. B.; Yang, Y.; Chen, J. H. Eur Polym J 2005, 41, 2742.
23. Weimer, M. W.; Fréchet, J. M. J.; Gitsov, I. J Polym Sci Part A: Polym Chem 1998, 36, 955.
24. Cao, Y.; Hong, Y.; Zhai, G. Q.; Zhang, D. L.; Song, Y.; Yu, Q.; Ren, Q.; Jiang, B. B. Polym Int 2008, 57, 1090.
25. Ren, Q.; Li, A. Y.; Jiang, B. B.; Zhang, D. L.; Chen, J. H. J Appl Polym Sci 2004, 94, 2425.
26. Li, A. Y.; Chang, J. Y.; Wang, K. Q.; Lu, L. D.; Yang, X. J.; Wang, X. Polym Int 2006, 55, 565.
27. Yang, Y. Z. M.S. Thesis, Jiangsu Polytechnic University, 2008.
28. Hay, A. S. Prog Polym Sci 1999, 24, 45.
29. Xu, T. W.; Liang, D. W. Prog Polym Sci 2008, 33, 894.
30. Puskas, J. E.; Kwon, Y. M.; Altstädt, V.; Kontopoulou, M. Polymer 2007, 48, 590.
31. Wang, X. D.; Feng, W.; Li, H. Q.; Ruckenstein, E. Polymer 2002, 43, 37.
32. Goh, S. H.; Zhang, J. W.; Lee, S. Y. Polymer 2000, 41, 8721.
33. Aroguz, A. Z.; Karasz, F. E. Polymer 2004, 45, 2685.
34. Liu, Q.; Shentu, B. Q.; Zhu, J. H.; Weng, Z. X. Eur Polym J 2007, 43, 890.
35. Li, Y. J.; Shimizu, H. Polymer 2004, 45, 7381.
36. Liu, W. B.; Kuo, W. F.; Chiang, C. J.; Chang, F. C. Eur Polym J 1996, 32, 91.
37. Hu, D. J.; Cheng, Z. P.; Wang, G.; Zhu, X. L. Polymer 2004, 45, 6525.
38. Paulo, C.; Puskas, J. E. Macromolecules 2001, 34, 734.
39. Chen, G. Q.; Wu, Z. Q.; Wu, J. R.; Li, Z. C.; Li, F. M. Macromolecules 2000, 33, 232.
40. Zhao, Y. L.; Zhang, J. M.; Jiang, J.; Chen, C. F.; Xi, F. J Polym Sci Part A: Polym Chem 2002, 40, 3360.
41. Jiang, X. L.; Xia, P.; Liu, W. L.; Yan, D. Y. J Polym Sci Part A: Polym Chem 20002, 38, 1203.
42. Lutz, J. F.; Kirci, B.; Matyjaszewski, K. Macromolecules 2003, 36, 3136.
43. Rzaev, Z. M. O. Prog Polym Sci 2000, 25, 163.
44. Liu, H. W.; Wilén, C. E. Macromolecules 2001, 34, 5067.
45. Wang, W. X.; Yan, D. Y.; Bratton, D.; Howdle, S. M.; Wang, Q.; Lecomte, P. Adv Mater 2003, 15, 1348.
46. Tang, W.; Matyjaszewski, K. Macromolecules 2007, 40, 1858.
47. Cai, Y. L.; Hartenstein, M.; Müller, A. H. E. Macromolecules 2004, 37, 7484.
48. Huang, J. Y.; Pintauer, T.; Matyjaszewski, K. J Polym Sci Part A: Polym Chem 2004, 42, 3285.
49. Bednarek, M.; Biedron, T.; Kubisa, P. Macromol Chem Phys 2000, 201, 58.
50. Xia, J. H.; Zhang, X.; Matyjaszewski, K. Macromolecules 1999, 32, 4482.
51. Moad, G.; Solomon, D. H. The Chemistry of Radical Polymerization, 2nd ed.; Elsevier Science: Oxford, 2006.
52. Jiang, B. B.; Fang, J. B.; Yang, Y.; Ren, Q.; Wang, W. Y.; Hao, J. J. Eur Polym J 2006, 42, 179.
53. Borman, C. D.; Jackson, A. T.; Bunn, A.; Cutter, A. L.; Irvine, D. J. Polymer 2000, 41, 6015.